



Discovery and biological evaluation of potent, selective, orally bioavailable, pyrazine-based blockers of the Na_v1.8 sodium channel with efficacy in a model of neuropathic pain

Marc J. C. Scanio^{a,*}, Lei Shi^a, Irene Drizin^a, Robert J. Gregg^a, Robert N. Atkinson^b, James B. Thomas^b, Matthew S. Johnson^b, Mark L. Chapman^b, Dong Liu^b, Michael J. Krambis^b, Yi Liu^b, Char-Chang Shieh^a, XuFeng Zhang^a, Gricelda H. Simler^a, Shailen Joshi^a, Prisca Honore^a, Kennan C. Marsh^a, Alison Knox^a, Stephen Werness^b, Brett Antonio^b, Douglas S. Krafte^b, Michael F. Jarvis^a, Connie R. Faltynek^a, Brian E. Marron^b, Michael E. Kort^a

^a Global Pharmaceutical Research and Development, Abbott Laboratories, Dept R4PM, Bldg. AP9A, 100 Abbott Park Road, Abbott Park, IL 60064-6117, United States

^b Icagen, Inc., 4222 Emperor Blvd., Durham, NC 27703, United States

ARTICLE INFO

Article history:

Received 13 July 2010

Revised 16 September 2010

Accepted 22 September 2010

Available online 29 September 2010

Keywords:

Sodium channels

Na_v1.8

PN3

Neuropathic pain

ABSTRACT

Na_v1.8 (also known as PN3) is a tetrodotoxin-resistant (TTx-r) voltage-gated sodium channel (VGSC) that is highly expressed on small diameter sensory neurons. It has been implicated in the pathophysiology of inflammatory and neuropathic pain, and we envisioned that selective blockade of Na_v1.8 would be analgesic, while reducing adverse events typically associated with non-selective VGSC blocking therapeutic agents. Herein, we describe the preparation and characterization of a series of 6-aryl-2-pyrazinecarboxamides, which are potent blockers of the human Na_v1.8 channel and also block TTx-r sodium currents in rat dorsal root ganglia (DRG) neurons. Selected derivatives display selectivity versus human Na_v1.2. We further demonstrate that an example from this series is orally bioavailable and produces antinociceptive activity *in vivo* in a rodent model of neuropathic pain following oral administration.

© 2010 Elsevier Ltd. All rights reserved.

1. Introduction

Voltage-gated sodium channels (VGSCs) are transmembrane proteins that open in response to changes in membrane potential to allow selective permeability of sodium ions.^{1–4} These channels belong to a multi-gene family consisting of nine members that are distinguished pharmacologically on the basis of their sensitivity to blockade by natural toxins, particularly tetrodotoxin (TTx).^{2,3} VGSCs contribute to the initiation and propagation of action potentials in excitable tissues such as nerve and muscle, and participate in many physiological processes including locomotion, cognition, and nociception.^{4–6}

Considerable data indicate that hyperexcitability and spontaneous action potential firing mediated by VGSCs in peripheral sensory neurons play a role in the pathophysiology of chronic

Abbreviations: TTx, tetrodotoxin; TTx-r, tetrodotoxin-resistant; VGSC, voltage gated sodium channels; DRG, dorsal root ganglia; ip, intraperitoneal; iv, intravenous; po, per os; F, bioavailability; T_{1/2}, half-life; Cl_p, plasma clearance; CEREP, cell-surface receptors, ion channels and enzymes; V_{ss}, volume of distribution at steady state; C_{max}, maximum concentration.

* Corresponding author. Tel.: +1 847 935 1064.

E-mail addresses: marc.scanio@abbott.com, mscanio@stanfordalumni.org (M.J.C. Scanio).

pain.^{7,8} Consistent with this hypothesis, non-selective blockade of sodium channels contributes to the analgesic activity of a number of clinically used agents, such as mexiletine, lamotrigine, and carbamazepine, all of which were developed for other indications. Unfortunately, the adverse events observed with these drugs limits their clinical utility for the treatment of chronic pain.⁹

Na_v1.8 (also known as PN3) is a TTx-resistant (TTx-r) VGSC that is preferentially expressed on sensory neurons¹⁰ and carries a major portion of the TTx-r current in peripheral nerves.¹¹ The highly localized distribution of Na_v1.8 in nociceptive small diameter neurons suggests this channel may be involved in the generation of action potentials in response to painful stimuli.¹² Increased expression of Na_v1.8 in chronic pain states,¹³ gene knockout data,^{14–16} and analgesic effects of Na_v1.8-specific antisense oligodeoxynucleotides^{17–19} support the premise that Na_v1.8 is an attractive target for analgesic drug discovery.^{20–23} Herein we describe a series of subtype-selective small molecule Na_v1.8 antagonists and their characterization as novel antihyperalgesic agents.

Our combined groups have previously disclosed the 5-aryl-2-furfuramides (Fig. 1) as potent and selective inhibitors of Na_v1.8.²⁴ A-803467, the most thoroughly characterized compound from the 5-aryl-2-furfuramides series, has excellent potency at recombinant human Na_v1.8 (IC₅₀ = 0.008 μM), inhibits TTx-r

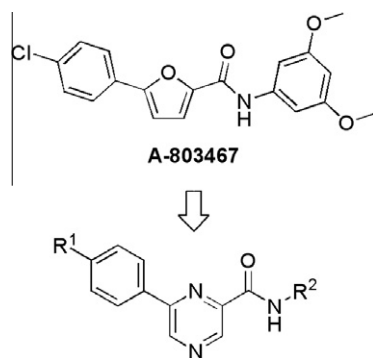
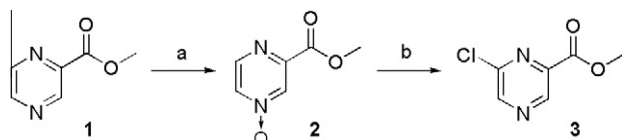


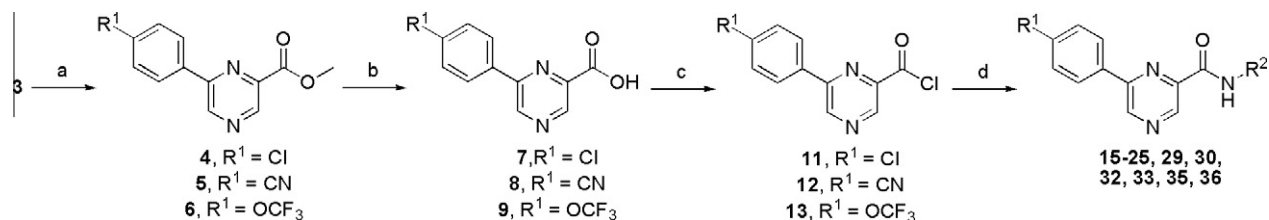
Figure 1. Expanding SAR by switching central cores.



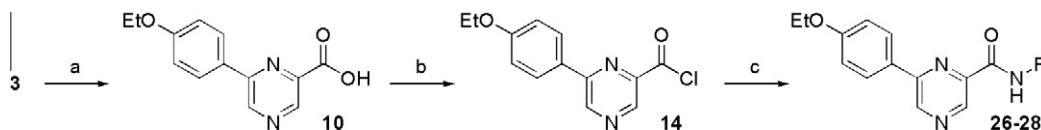
Scheme 1. Conditions: (a) *m*CPBA, 1,2-dichloroethane; (b) SOCl_2 .

currents ($\text{IC}_{50} = 0.14 \mu\text{M}$) in rat DRG neurons and is selective versus other sodium channels ($\text{Na}_v1.2$, $\text{Na}_v1.3$, $\text{Na}_v1.5$, $\text{Na}_v1.7$) and the hERG channel.^{25,26,34} It is active in Chung ($\text{EC}_{50} = 47 \text{ mg/kg}$), Bennett ($\text{EC}_{50} = 85 \text{ mg/kg}$), and CFA ($\text{EC}_{50} = 41 \text{ mg/kg}$) rodent models of pain following intraperitoneal (ip) administration, and is now commercially available as a tool compound. A-803467 has low oral bioavailability ($F = 13\%$ at 10 mg/kg) in rat, moderate in vitro intrinsic clearance ($140 \mu\text{L min}^{-1} \text{ mg}^{-1}$, rat microsomes) and lacks linear increases in plasma exposure upon escalating oral dose, presumably due to solubility limited absorption (aqueous solubility $< 0.1 \mu\text{g/mL}$).²⁷

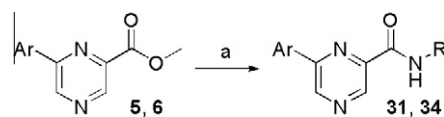
We were interested in evaluating other central core series in an attempt to identify new compounds with improved aqueous solubility and oral bioavailability relative to the furan series, while maintaining or improving potency (Fig. 1). Pyridine, oxazole, thiazole, oxadiazole, thiazole and thiadiazole central core replacements have recently been reported.²⁷ As a continuing part of this strategy, pyrazine derivatives were synthesized and found to possess encouraging levels of $\text{Na}_v1.8$ potency and isoform selectivity. These preliminary findings set the stage for a more detailed SAR investigation of 6-aryl-2-pyrazinecarboxamide derivatives, the syntheses of which are detailed in Schemes 1–4.



Scheme 2. Conditions: (a) $\text{ArB}(\text{OH})_2$, $\text{PdCl}_2(\text{PPh}_3)_2$, Cs_2CO_3 , DMF; (b) NaOH , $\text{H}_2\text{O}/\text{EtOH}$; (c) $(\text{COCl})_2$, cat. DMF, CH_2Cl_2 ; (d) H_2NR , TEA, CH_2Cl_2 .



Scheme 3. Conditions: (a) 4-ethoxyphenylboronic acid, $\text{PdCl}_2(\text{PPh}_3)_2$, Na_2CO_3 , $\text{iPrOH}/\text{H}_2\text{O}$; (b) $(\text{COCl})_2$, cat. DMF, CH_2Cl_2 ; (c) H_2NR , TEA, CH_2Cl_2 .



Scheme 4. Conditions: (a) H_2NR , MgCl_2 , THF.

2. Chemistry

Methyl 6-chloro-2-pyrazinecarboxylate (**3**)^{28,29} served as an intermediate for our exploration of 6-substituted 2-pyrazinecarboxamides and could be readily prepared in two steps on multigram scale (Scheme 1). 4-Oxo-2-pyrazinecarboxylate (**2**) was formed by oxidation of methyl pyrazinecarboxylate (**1**) with *m*CPBA.³⁰ *N*-Oxide **2** was then refluxed in thionyl chloride to afford the key intermediate **3**.³¹ The regiochemistry of **3** is consistent with literature precedence,³¹ and was confirmed by an HMBC NMR experiment, which showed a long-range correlation between H5 and C3, indicating that the ester and chloro substitutions are at the 2- and 6-positions.

The majority of analogs for this study were synthesized by the route illustrated in Scheme 2. Suzuki coupling of aryl boronic acids and **3** afforded methyl 6-aryl-2-pyrazinecarboxylates **4–6**. The methyl esters were saponified to carboxylic acids **7–9** and subsequently converted to acid chlorides **11–13**. A variety of amide analogs (**15–25**, **29**, **30**, **32**, **33**, **35** and **36**) were prepared by reacting **11–13** with amines in the presence of triethylamine.

Under the aqueous conditions used in the Suzuki coupling of 4-ethoxyphenylboronic acid to **3** (Scheme 3), the ester functionality underwent hydrolysis to provide carboxylic acid **10**. Compound **10** was subsequently converted to amide analogs **26–28** via acid chloride **14**. An alternative method for amide formation involved direct conversion of esters **5** and **6** to amides **31** and **34**, respectively, mediated by MgCl_2 (Scheme 4).³²

3. Biological evaluation

All compounds were first evaluated for the ability to block the recombinant mouse $\text{Na}_v1.8$ ($\text{mNa}_v1.8$) sodium channel stably expressed in HEK293 cells using a modified version of an isotopic efflux assay.³³ The activity of selected compounds was confirmed by demonstrating inhibition of sodium currents in human $\text{Na}_v1.8$ ($\text{hNa}_v1.8$) expressing HEK293 cells using a conventional voltage-clamp electrophysiology procedure.²⁵ Electrophysiological evaluation of inhibition of native TTX-r sodium current in acutely dissociated DRG neurons was carried out for a subset of these

compounds.^{24,25} Screening against human Na_v1.2 provided an assessment of VGSC subtype selectivity. Inhibition of the hERG channel was also evaluated as a potential liability.³³ All of the final compounds, **15–36**, demonstrated hERG IC₅₀ >10 μM, which was not considered to be a major liability. Selected compounds were evaluated for aqueous solubility. Key compounds were also evaluated for in vitro microsomal stability in rat microsomes.

Electrophysiological protocols were designed to set the membrane potential to the midpoint of voltage-dependent steady-state inactivation (i.e., the voltage at which 50% of channels are inactivated or V_{1/2}): V_{1/2} = −40 mV for hNa_v1.8, TTx-r; V_{1/2} = −60 mV for hNa_v1.2. For each channel, compounds were evaluated at 1–3 concentrations, with 2–6 measurements at each concentration. For compounds with multiple single-point data, the average of the various estimated values is reported.

Following an assessment of the pharmacokinetic profile, candidate compounds were further evaluated in the L5/L6 spinal nerve tight ligation (Chung)^{18,35,40} model of neuropathic pain.

4. Results and discussion

Initially, we chose to examine 6-(4-chlorophenyl)pyrazine-2-carboxamides (Table 1) based on our SAR experience with the related furan series,²⁴ wherein 4-chlorophenyl substitution generally led to potent Na_v1.8 inhibitors. Compounds with an IC₅₀ value <3 μM in the mNa_v1.8 flux assay were advanced for additional, more rigorous electrophysiological evaluation; compounds with an IC₅₀ value >3 μM in the mNa_v1.8 flux assay generally showed poor activity in electrophysiological evaluation of hNa_v1.8 or TTx-r. We elected to use the recombinant mouse Na_v1.8 cell line for compound triage because of concerns with intellectual property. In general, compounds displaying the most potent activity in the recombinant mouse were among the most potent blockers in the recombinant human assay. It is unclear to us whether the observed left-shift in potency observed in the hNav1.8 assay derives from a species difference (mouse vs human) or a screening platform difference (flux vs electrophysiological evaluation).

The anilides (**15–17**) were the first compounds to be evaluated. These analogs were inhibitors in the mNa_v1.8 flux assay, with IC₅₀ values <2 μM in all cases. In electrophysiological assays, the anilides were very potent inhibitors (IC₅₀ <10 nM) of hNa_v1.8. The anilides also demonstrated good TTx-r inhibition (IC₅₀ <300 nM) and generally had favorable selectivity (>1000-fold) for hNa_v1.8 versus Na_v1.2. For example, the most potent anilide, **17**, was a 3 nM hNa_v1.8 blocker (TTx-r IC₅₀ 52 nM) and >1600-fold selectivity against Na_v1.2. The benzyl amine **18** maintained comparable potency relative to the anilides in the mNa_v1.8 flux, hNa_v1.8 and TTx-r assays and showed excellent selectivity against Na_v1.2 (<5% inhibition at 3 μM). Further extension of the linker between the amide and aromatic group to phenethylamine derivative **19** resulted in conserved in vitro potency in the hNa_v1.8 and TTx-r assays, but with a substantial loss of selectivity against Na_v1.2 (53-fold selective). Therefore we elected to focus the majority of our effort on exploring the SAR of anilides, benzyl amides and their heterocyclic analogs.

As the simple anilides tended to be very water insoluble (e.g., the aqueous solubility of **17** <0.1 μg/mL), steps were taken to increase water solubility by incorporating heteroatoms, such as in pyridyl analog **20** and in 2-picolinyl derivative **21**. Although the potency of **21** was weak, its increased aqueous solubility (1 μg/mL) was a 10-fold improvement relative to **17** making it an attractive starting point for the design of compounds with enhanced physiochemical properties. In analog **22**, for example, the objective was to attenuate the basicity of the pyridine nitrogen, which we thought might be

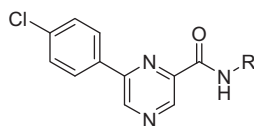
responsible for the loss of potency, while incorporating a water solubilizing morpholino group. Compound **22** (aqueous solubility = 2.7 μg/mL) was potent at Na_v1.8 and TTx-r, while maintaining selectivity versus Na_v1.2. Perturbing the position of the pyridine nitrogen, as in isomers **23** and **24** led to a dramatic loss of Na_v1.8 potency. Replacing the morpholino group of **22** with a pyrrolidino in compound **25** resulted in a compound with comparable potency at hNa_v1.8 and TTx-r, but less selectivity versus Na_v1.2 and lower aqueous solubility than either **21** or **22** (Table 1). The in vitro turnover of **22** was high (410 μL min^{−1} mg^{−1}, rat microsomes) prompting us to look for compounds with both improved solubility and stability.

We next examined various aromatic substitutions with anilides, benzyl amides and their heterocyclic analogs (Table 2). The 4-ethoxy, 4-cyano and 4-trifluoromethoxy aromatic substitutions were selected in an attempt to improve the overall solubility and stability of these compounds. The 4-ethoxyphenyl derivatives **26–28** were very potent at both Na_v1.8 and TTx-r. Collectively, however, they possessed greater activity against Na_v1.2 (IC₅₀ ≤1 μM), and the ethoxy group presented a potential metabolic liability. For example, **28** proved particularly susceptible to microsomal turnover (630 μL min^{−1} mg^{−1}, rat microsomes). The 4-cyanophenyl 3,5-dimethylanilide analog **29**, maintained the high Na_v1.8 and TTx-r potency of other 3,5-dimethylanilide derivatives, such as **17**, **26** and **32**. This activity did not, however, extend to the other 4-cyanophenyl derivatives, **30** and **31**, which showed weaker TTx-r potency (IC₅₀ >100 nM). Compound **29** had modest in vitro intrinsic clearance (140 μL min^{−1} mg^{−1}, rat microsomes), but had poor aqueous solubility (0.03 μg/mL) and no oral bioavailability. The 4-trifluoromethoxy derivatives **32–36** tended toward good potency at both Na_v1.8 and TTx-r. Morpholine **36** was designed to mimic the solubilizing strategy used in **22**, and was also more potent at Na_v1.8 and TTx-r than **22**. In fact, **36** was markedly more water soluble (>50 μg/mL) than the other compounds in this series. In addition, **36** had modest in vitro intrinsic clearance (98 μL min^{−1} mg^{−1}, rat microsomes). Compound **36** was more active at Na_v1.2 than **22**, but its IC₅₀ was greater than 1 μM and was still 79-fold selective relative to hNa_v1.8.

Given its improved aqueous solubility and favorable clearance values, **36** was selected for pharmacokinetic evaluation (Table 3), where it demonstrated modest oral bioavailability and exposure. Oral administration of **36** resulted in dose-dependent attenuation of mechanical allodynia in the L5/L6 spinal nerve injury (Chung) model of neuropathic pain (ED₅₀ = 78 mg/kg) (Fig. 2). A comparison of **36** and **29** demonstrates the importance of physiochemical properties in this series, as the two compounds had similar potency at Na_v1.8, TTx-r and Na_v1.2. Compound **36** was much more water soluble than **29** (>50 μg/mL vs 0.03 μg/mL), supporting the hypothesis that increasing solubility would increase exposure and oral activity. Compounds **36** and **29** were also tested in a broad screening panel (N = 70) of cell-surface receptors, ion channels and enzymes (CEREP, Poitiers, France) and showed no or weak (IC₅₀ >2 μM) activity, **36** showed modest activity at three receptors at 10 μM (Table 3).

5. Conclusion

We have identified a novel series of pyrazine-based derivatives that are potent, selective blockers of the Na_v1.8 sodium channel. These compounds further demonstrate that the furan core of A-803467 can be replaced with heteroaromatics, while maintaining potency at blocking Na_v1.8 channels and DRG neurons.²⁷ In general, good activity was achieved with a variety of substitutions on the general pyrazine scaffold but with different SAR from the

Table 1In vitro characterization of 6-(4-chlorophenyl)pyrazine-2-carboxamide Na_v1.8 channel blockers **15–25** and A-803467 for comparison

Compound	R	mNa _v 1.8 IC ₅₀ (μM)	hNa _v 1.8 Est. IC ₅₀ ^a (μM)	TTX-r Est. IC ₅₀ ^a (μM)	hNa _v 1.2 Est. IC ₅₀ ^a (μM)	Solubility (μg/mL)	Rat microsomal clearance (μL/min/mL)
A-803467		0.85 ± 0.3 ^b	0.008 ^b	0.14 ^b	7.4 ^b	<0.1 ^d	140 ^d
15		1.07 ± 0.34	0.006	0.19	6.2	<0.1	
16		0.96 ± 0.20	0.006	0.28	8.2	<0.1	
17		0.49 ± 0.30	0.003	0.052	5.0	<0.1	83
18		1.34 ± 0.12	0.027	0.11	2% @ 3 μM ^c	<0.1	
19		2.68 ± 0.46	0.019	0.36	1.0	<0.1	
20		18 ± 2.0					
21		11 ± 1.48				1.0	
22		2.50 ± 0.25	0.037	0.28	11% @ 3 μM ^c	2.7	410
23		4.14 ± 2.29	0.32				
24		29.1 ± 3.0					
25		0.21 ± 0.09	0.030	0.55	1.0	0.65	

^a Estimated IC₅₀ values from electrophysiology data generated at multiple testing concentrations (see Section 6.7).^b Data from Ref. 25.^c Percent inhibition of hNa_v1.2 at 3 μM.^d Data from Ref. 27.

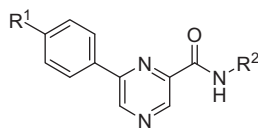
furans core. The physicochemical and pharmacokinetic properties of many of these compounds limited the in vivo evaluation of their analgesic profiles. However, consistent with its in vitro profile and improved solubility, the oral administration of **36** produced dose-dependent anti-nociceptive effects in a rodent model of neuropathic pain.

6. Experimental section

6.1. General procedures

Nuclear magnetic resonance spectra were obtained on a 300, 400, or 500 MHz instruments with chemical shifts (δ) reported rel-

Table 2
In vitro characterization of pyrazine Na_v1.8 channel blockers **26–36**



Compound	R ¹	R ²	mNa _v 1.8 IC ₅₀ (μM)	hNa _v 1.8 Est. IC ₅₀ ^a (μM)	TTx-r Est. IC ₅₀ ^a (μM)	hNa _v 1.2 Est. IC ₅₀ ^a (μM)	Solubility (μg/mL)	Rat microsomal clearance (μL/min/mL)
26	-OEt		0.056 ± 0.1	0.002	0.012	0.36	<0.1	
27	-OEt		0.65 ± 0.13	0.001	0.068	1.0	<0.1	
28	-OEt		0.11 ± 0.05	0.002	0.019	0.47	0.14	630
29	-CN		0.47 ± 0.07	0.008	0.084	1.6	0.03	140
30	-CN		0.73 ± 0.28	0.049	0.13	9.1	0.08	120
31	-CN		9.4 ± 8	0.15	0.45	1.0	0.35	
32	-OCF ₃		0.058 ± 0.05	0.021	0.034	93% @ 3 μM ^b	<0.1	
33	-OCF ₃		0.066 ± 0.05	0.005	0.016	2.2	<0.1	
34	-OCF ₃		0.24 ± 0.06	0.018	0.17	1.2		
35	-OCF ₃		1.03 ± 0.4	0.099	0.090	3.9		143
36	-OCF ₃		0.48 ± 0.09	0.019	0.085	1.5	>50	98

^a Estimated IC₅₀ values from electrophysiology data generated at multiple testing concentrations (see Section 6.7).

^b Percent inhibition of hNa_v1.2 at 3 μM

ative to tetramethylsilane as internal standard. Mass spectra determinations were obtained using an electrospray (ESI) technique or by direct chemical ionization (DCI) methods employing ammonia. Melting points were determined with capillary apparatus and are uncorrected. Elemental analyses were performed by Robertson Microlit Laboratories, Inc., Madison, NJ. Analytical thin layer chromatography was done on 2 × 6 cm Kieselgel 60 F-254 plates pre-coated with 0.25 mm thick silica gel distributed by E. Merck. LC–MS analyses were performed on ThermoQuest Navigator systems using 10–100% acetonitrile:10 mM ammonium acetate gradient with MS data obtained using atmospheric pressure chemical ionization (APCI) positive ionization over the range of *m/z* from 170 to 1200. Unless otherwise specified, column chromatography

was performed on silica gel (230–400 mesh). The term *in vacuo* refers to solvent removal using a rotary evaporator. Unless otherwise specified, solvents and reagents were purchased from Aldrich Chemical Co. and were used without further purification unless otherwise specified.

6.2. High-throughput mouse Na_v1.8 and hERG isotopic flux assays

HEK293 cells stably expressing mouse Na_v1.8 sodium channels or CHO cells stably expressing hERG potassium channels were loaded overnight with an appropriate radiotracer, followed by stimulation using variations on protocols previously described.^{33,36}

Table 3
In vivo activity^a and pharmacokinetic profile^b of Na_v1.8 blockers **36** and **29**

	36	29
Neuropathic pain, Chung po (ED ₅₀ , mg/kg)	78	<20% @ 100 μM ^c
F, po (%)	18.2 ± 2.5	0%
Cl _p (L/(h kg))	2.04 ± 0.10	2.0
T _{1/2} (h)	1.9 (iv) 1.6 (po)	1.6 (iv)
C _{max} , po (μg/mL)	0.15 ± 0.03	0
iv V _{ss} (L/kg)	3.3 ± 0.3	5.1
Plasma protein binding, rat (%)	93.2 ± 0.4	55.2 ± 1.6
Cerep (@ 10 μM) ^d	β ₂ (h), BZD	None
	peripheral, NK ₁ (h)	

^a Values shown represent the mean for experiments in rats, *n* = 6 per dose group.

^b Pharmacokinetic parameters determined in rats (*n* = 3) following administration of a 3 mg/kg iv or po dose.

^c Percent inhibition at 100 μM.

^d Displayed >60% inhibition of control specific binding at indicated receptor.

The radiotracer efflux was measured at a single time point which had been previously established to be on the linear portion of the efflux curve. Percentage inhibition of efflux was calculated as:

$$\% \text{ inhibition} = 1 - \frac{[\text{Efflux}(\text{test compound}) - \text{Efflux}(\text{ref blocker})]}{[\text{Efflux}(\text{Control}) - \text{Efflux}(\text{ref blocker})]} \times 100$$

Reference blockers for Na_v1.8 and hERG assays were tetracaine (30 μM) and terfenadine (30 μM), respectively. Concentration dependent activity was established via eight-point concentration–response curves and assays were performed in duplicate.

6.3. Electrophysiology. Recombinant human sodium channels²⁵

Human embryonic kidney (HEK-293) cells expressing recombinant sodium channels were grown in DMEM/High Glucose Dul-

becco's media, 10% Fetal Bovine Serum, 2 mM sodium pyruvate, G418. For whole-cell voltage-clamp recordings, patch pipettes were pulled from borosilicate glass on a Flaming–Brown micropipette puller (Sutter Instruments, Inc). Pipettes had a tip resistance of 0.8–2.5 MΩ using the internal solutions (mM): 135 CsF, 10 CsCl, 5 EGTA, 5 NaCl, 10 HEPES-free acid, pH to 7.3 with 5 M CsOH and voltage offset was zeroed prior to seal formation. The external buffer consisted of (mM): 132 NaCl, 5.4 KCl, 0.8 MgCl₂, 1.8 CaCl₂, 5 Glucose, 10 HEPES-free acid, pH to 7.3 with 6 N NaOH. After establishment of a whole-cell recording, cellular capacitance was minimized using the analog compensation available on the recording amplifier (Axopatch 200B). Series resistance was less than 5 MΩ and was compensated >85% in all experiments, resulting in a final series resistance no greater than 0.75 MΩ. Signals were low-pass filtered at 5–10 kHz, digitized at 20–50 kHz, and stored on a computer for later analysis. Voltage protocols were generated and data acquisition and analysis were performed using pCLAMP software (Version 8.1, Axon Instruments, Inc.). All experiments were performed at room temperature. Liquid junction potentials were <10 mV and were not corrected.

6.4. Electrophysiological recordings. Rat dorsal root ganglion neurons^{37,38}

Whole-cell patch clamp recordings were performed on dissociated rat small diameter DRG neurons (18–25 μm) from the L4 and L5 lumbar region at room temperature. Coverslips were mounted in a small flow-through chamber on the stage of an inverted microscope and were continuously perfused with bath external solution (see below). Cells were voltage clamped via the whole-cell configuration of the patch clamp with an Axopatch-200B amplifier (Molecular Devices/Axon Instruments, Foster City, CA) using standard techniques. Micropipettes were pulled from thin-walled borosilicate glass capillaries (TW-150F, World Precision Instruments, Sarasota, FL) with a Flaming–Brown micropipette puller (P97, Sutter Instrument, Novato, CA) and polished on a microforge

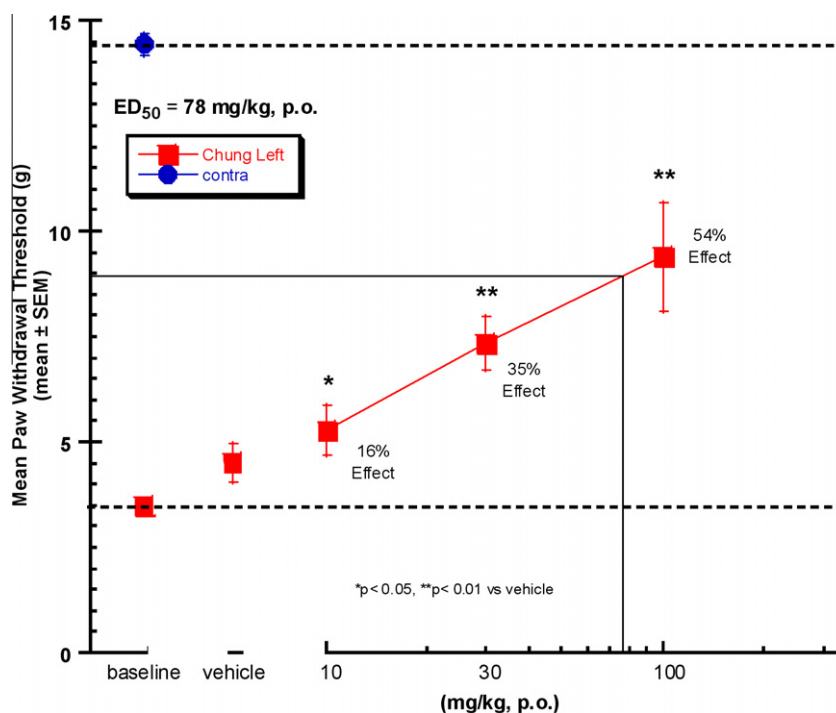


Figure 2. Effects of **36** on mechanical allodynia observed in the Chung model of neuropathic pain (*n* = 6). Compound was administered (10, 30, 100 mg/kg po) 60 min before von Frey testing. Squares represent paw withdraw threshold ipsilateral to the injury (left). The circle represents paw withdrawal threshold contralateral to the injury. Data represent mean ± SEM. *, significantly different (*P* < 0.05) from vehicle-treated animals (*n* = 6); **, significantly different (*P* < 0.01) from vehicle-treated animals (*n* = 6).

(Narishige, Tokyo) to obtain electrode resistances ranging from 1.0–2.5 M Ω . The pipette solution contained (mM): 135 CsF, 5 NaCl, 10 HEPES, 10 CsCl, and 5 EGTA, pH 7.4 with CsOH (295 mOSM). Capacity transients were cancelled and series resistance was compensated (>80%) using the facilities of the amplifier. The bath solution contained (mM): 110 choline-Cl, 22 NaCl, 5.4 KCl, 1.8 CaCl₂, 0.8 MgCl₂, 10 HEPES, and 5 glucose, plus 500 nM tetrodotoxin (TTx) and 50 μ M CdCl₂, pH 7.4 with NaOH (300 mOSM). The pipette potential was zeroed before seal formation. Calculated liquid junction potentials were \leq 5 mV and were not corrected. Whole-cell currents were filtered at 5 kHz and acquired at 20 kHz using Clampex 8.2 software (Molecular Devices/Axon Instruments) and analyzed using Clampfit 8.2 (Molecular Devices/Axon Instruments). All experiments were performed at room temperature (21–25 °C). Compounds were dissolved in DMSO (10 mM) and added to extracellular solution (final DMSO concentration <0.1%) immediately prior to use. Compounds were applied directly to the voltage-clamped cells at a flow rate of 1–2 mL/min via a custom-made perfusion manifold connected to an array of gravity-fed reservoirs. Sodium currents were evoked from a holding potential of –100 mV by a test pulse of 0 mV for 20 ms and pulsed every 15 s until stabilized. To measure drug effects, sodium currents were evoked with 20 ms steps to 0 mV following 8 s prepulses to either –100 mV or –40 mV. The prepulse was followed by a brief (20 ms) repolarization to –100 mV to relieve fast inactivation.

6.5. In vivo evaluation

Male Sprague–Dawley rats (Charles River, Wilmington, MA) weighing 200–300 g were utilized. All animals were group housed in AAALAC approved facilities at Abbott Laboratories in a temperature-regulated environment with lights on between 0700 and 2000 h. Food and water were available ad libitum except during testing. All animal handling and experimental protocols were approved by an institutional animal care and use committee (IACUC). All experiments were performed during the light cycle. Unless otherwise noted, all experimental and control groups contained at least six animals per group and data are expressed as mean \pm SEM. Data analysis was conducted using analysis of variance and appropriate post-hoc comparisons ($P < 0.05$) as previously described.³⁹ ED₅₀ values were estimated using least squares linear regression.

6.6. Spinal nerve (L5/L6) ligation model of neuropathic pain

As previously described in detail by Kim and Chung,⁴⁰ a 1.5 cm incision was made dorsal to the lumbosacral plexus in anesthetized rats. The paraspinal muscles (left side) were separated from the spinous processes, the L5 and L6 spinal nerves were isolated and tightly ligated with 3–0 silk threads. Following hemostasis, the wound was sutured and coated with antibiotic ointment. The rats were allowed to recover and then placed in a cage with soft bedding for 14 days before behavioral testing for mechanical allodynia. The vehicle for compound administration and vehicle control animals was 10% DMSO in PEG400. Paw withdraw threshold was determined with von Frey hairs and reported as mean \pm SEM.

6.7. Estimated IC₅₀ values

Estimated IC₅₀ values were calculated from single-point electrophysiology data using the following equation: [(100% – % inhibition)/% inhibition] \times (test concentration in μ M). Inhibition values <20% and >80% are excluded from the calculation. For compounds with multiple single-point data, the average of the various estimated values was reported. Data were collected using an inactivated state protocol (the prepulse voltage at which 50% of

channels are inactivated. $V_{1/2} = -40$ mV for hNa_v1.8, TTx-r; $V_{1/2} = -60$ mV for hNa_v1.2.

6.7.1. Methyl 4-oxy-2-pyrazinecarboxylate (2)

Methyl 2-pyrazinecarboxylate (1) (Pyrazine Specialists, 10.04 g, 72.2 mmol) was suspended in 1,2-dichloroethane (100 mL). To the reaction mixture was added *m*CPBA (32.35 g, 77%, 144 mmol). The reaction mixture was stirred at 60 °C for 16 h, then allowed to cool to ambient temperature and diluted with CH₂Cl₂ (300 mL). The precipitate was filtered off and washed with additional CH₂Cl₂ (3 \times 35 mL). The filtrates were combined, dried over K₂CO₃, filtered and concentrated. The residue was suspended in hexane (50 mL). The title compound was isolated by filtration, washed with additional hexane (2 \times 50 mL) to afford a slightly yellow solid (7.22 g, 64%): ¹H NMR (DMSO-*d*₆, 300 MHz) δ 3.91 (s, 3H), 8.54 (dd, $J = 4.07, 1.69$ Hz, 1H), 8.64–8.67 (m, 2H) ppm. ¹³C NMR (DMSO-*d*₆, 100 MHz) δ 53.0, 135.2, 136.2, 147.1, 148.8, 162.68 ppm; MS (DCI/NH₃) m/z 155 (M+H)⁺; Anal. (C₆H₆N₂O₃) C, H, N.

6.7.2. Methyl 6-chloro-2-pyrazinecarboxylate (3)

Methyl 4-oxy-2-pyrazinecarboxylate (2) (7.18 g, 45.9 mmol) was dissolved in SOCl₂ (50 mL, 687 mmol). The reaction mixture was heated to reflux for 8 h and then allowed to cool to ambient temperature. The SOCl₂ was removed under reduced pressure, and the residue was quenched with water (50 mL) at 0 °C. The mixture was neutralized by the addition of 1 M K₂CO₃ (aq) and extracted with CH₂Cl₂ (5 \times 100 mL). The organic extracts were combined and washed with brine (100 mL), dried over Na₂SO₄, filtered and concentrated. The residue was purified by silica gel chromatography (5% EtOAc in CH₂Cl₂, $R_f = 0.35$) to afford the title compound as a thick oil that slowly solidified (7.16 g, 67%): ¹H NMR (DMSO-*d*₆, 500 MHz) δ 3.95 (s, 3H), 9.07 (s, 1H), 9.18 (s, 1H) ppm; ¹³C NMR (DMSO-*d*₆, 125 MHz) δ 52.9, 142.1, 143.6, 144.9, 148.1, 162.8 ppm; MS (DCI/NH₃) m/z 190 (M+NH₄)⁺; Anal. (C₆H₅ClN₂O₂) C, H, N.

6.7.3. Representative procedure for Suzuki coupling (Scheme 2, step a). Methyl 6-(4-chlorophenyl)-2-pyrazinecarboxylate (4)

Methyl 6-chloro-2-pyrazinecarboxylate (3) (1.01 g, 5.85 mmol) was dissolved in DMF (23 mL). 4-Chlorophenylboronic acid (1.34 g, 8.57 mmol), PdCl₂(PPh₃)₂ (204.5 mg, 0.29 mmol) and cesium carbonate (4.44 g, 13.63 mmol) were added, and the reaction mixture was stirred at 65 °C for 16 h. The reaction mixture was then diluted with water (200 mL) and extracted with EtOAc (3 \times 100 mL). The organic extracts were combined, washed with water (2 \times 100 mL) and brine (200 mL), dried over Na₂SO₄, filtered and concentrated. The residue was purified by silica gel chromatography (5% EtOAc in CH₂Cl₂, $R_f = 0.39$) to afford the title compound as a white solid (789.7 mg, 54%): ¹H NMR (DMSO-*d*₆, 300 MHz) δ 3.97 (s, 3H), 7.65–7.68 (m, 2H), 8.23–8.25 (m, 2H), 9.17 (s, 1H), 9.52 (s, 1H) ppm. MS (DCI/NH₃) m/z 249 (M+H)⁺.

6.7.3.1. Methyl 6-(4-cyanophenyl)-2-pyrazinecarboxylate (5).

Yield 51%; ¹H NMR (DMSO-*d*₆, 300 MHz) δ 3.98 (s, 3H), 8.05–8.09 (m, 2H), 8.37–8.41 (m, 2H), 9.24 (s, 1H), 9.61 (s, 1H) ppm; MS (DCI/NH₃) m/z 240 (M+H)⁺.

6.7.3.2. Methyl 6-(4-trifluoromethoxyphenyl)-2-pyrazinecarboxylate (6). Yield 61%; ¹H NMR (DMSO-*d*₆, 300 MHz) δ 3.97 (s, 3H), 7.57–7.60 (m, 2H), 8.31–8.36 (m, 2H), 9.19 (s, 1H), 9.53 (s, 1H) ppm; MS (DCI/NH₃) m/z 299 (M+H)⁺.

6.7.4. Representative procedure for ester saponification (Scheme 2, step b). 6-(4-Chlorophenyl)-pyrazine-2-carboxylic acid (7)

Methyl 6-(4-chlorophenyl)-2-pyrazinecarboxylate (4) (764.5 mg, 3.07 mmol) was suspended in EtOH (15 mL). 1 M NaOH (15 mL)

was added, and the reaction mixture stirred at ambient temperature for 1 h. The reaction mixture was acidified to pH \approx 3 with 1 M HCl (aq). The mixture was then diluted with water (100 mL) and extracted with EtOAc (5 \times 50 mL). The organic extracts were combined, washed with brine (100 mL), dried over Na₂SO₄, filtered and concentrated to provide the title compound as a white solid (715.1 mg, 99%): ¹H NMR (DMSO-*d*₆, 300 MHz) δ 7.63–7.67 (m, 2H), 8.24–8.29 (m, 2H), 9.15 (s, 1H), 9.49 (s, 1H), 13.82 (br s, 1H) ppm; MS (DCI/NH₃) *m/z* 235 (M+H)⁺.

6.7.4.1. 6-(4-Cyanophenyl)-pyrazine-2-carboxylic acid (8). Yield 98%; ¹H NMR (DMSO-*d*₆, 300 MHz) δ 8.06 (d, *J* = 8.48 Hz, 2H), 8.43 (d, *J* = 8.48 Hz, 2H), 9.21 (s, 1H), 9.58 (s, 1H), 13.89 (br s, 1H) ppm; MS (DCI/NH₃) *m/z* 226 (M+H)⁺.

6.7.4.2. 6-(4-Trifluoromethoxyphenyl)-pyrazine-2-carboxylic acid (9). Yield 99%; ¹H NMR (DMSO-*d*₆, 300 MHz) δ 7.57–7.59 (m, 2H), 8.34–8.37 (m, 2H), 9.16 (s, 1H), 9.50 (s, 1H), 13.82 (br s, 1H) ppm; MS (DCI/NH₃) *m/z* 285 (M+H)⁺.

6.7.5. 6-(4-Ethoxyphenyl)-pyrazine-2-carboxylic acid (10)

Methyl 6-chloro-2-pyrazinecarboxylate (**3**) (440 mg, 2.55 mmol) was dissolved in 75% aqueous isopropanol solution (50 mL). 4-Ethoxyphenylboronic acid (487 mg, 2.93 mmol), PdCl₂(PPh₃)₂ (72 mg, 0.10 mmol) and sodium carbonate (676 mg, 6.37 mmol) were added, and the reaction mixture was stirred at refluxing temperature for 4 h. The reaction mixture was then diluted with ethyl acetate (100 mL) and was partitioned between ethyl acetate (100 mL) and water (250 mL). The organic layer was washed with 2 M NaOH (100 mL). The aqueous layers were combined and acidified to pH 2–3. The acidified aqueous layer was extracted with ethyl acetate (2 \times 150 mL). The organic extracts were combined, dried over Na₂SO₄, filtered and concentrated in vacuo to afford the desired product as an off-white solid (600 mg, 96%): ¹H NMR (MeOH-*d*₄, 400 MHz) δ 1.42 (t, *J* = 7.1 Hz, 3H), 4.13 (q, *J* = 7.0 Hz, 2H), 7.00–7.15 (m, 2H), 8.11–8.17 (m, 2H), 9.07 (s, 1H), 9.22 (s, 1H) ppm; MS (APCI) *m/z* 245 (M+H)⁺.

6.7.6. Representative procedure for acid chloride formation (Scheme 2, step c). 6-(4-Cyanophenyl)-pyrazine-2-carbonyl chloride (12)

6-(4-Cyanophenyl)-pyrazine-2-carboxylic acid (**8**) (1.36 g, 6.04 mmol) was suspended in dichloromethane (60 mL). Oxalyl chloride (0.95 mL, 10.89 mmol) and DMF (30 μ L, 0.31 mmol) were added, and the reaction mixture was stirred at ambient temperature for 1 h. The mixture was concentrated and placed under high vacuum to provide the crude product (1.45 g, 99%), which was used without additional purification.

6.7.6.1. 6-(4-Chlorophenyl)-pyrazine-2-carbonyl chloride (11). Yield 95%.

6.7.6.2. 6-(4-Trifluoromethoxyphenyl)-pyrazine-2-carbonyl chloride (13). Yield 99%.

6.7.6.3. 6-(4-Ethoxyphenyl)-pyrazine-2-carbonyl chloride (14). Yield 95%.

6.7.7. Representative procedure for amide formation from acid chlorides (Scheme 2, step d). *N*-(3-Isopropoxyphenyl)-6-(4-cyanophenyl)-pyrazine-2-carboxamide (29)

6-(4-Cyanophenyl)-pyrazine-2-carbonyl chloride (**12**) (394.4 mg, 1.62 mmol) was dissolved in dichloromethane (16 mL). Triethylamine (0.33 mL, 2.37 mmol) and 3-isopropoxyaniline (0.36 mL, 2.44 mmol) were added, and the reaction mixture was stirred at ambient temperature for 3 h. The mixture was then poured into

0.1 M HCl (100 mL) and extracted with CH₂Cl₂ (3 \times 50 mL). The organic extracts were combined, washed with 0.1 M HCl (50 mL) and brine (50 mL), dried over Na₂SO₄, filtered and concentrated. The residue was purified by silica gel chromatography (10% EtOAc in CH₂Cl₂, *R*_f = 0.26) to afford the title compound as a white solid (391.0 mg, 67%): mp 161–162 °C; ¹H NMR (DMSO-*d*₆, 300 MHz) δ 1.30 (d, *J* = 5.76 Hz, 6H), 4.57–4.65 (m, 1H), 6.75 (dd, *J* = 7.80, 2.03 Hz, 1H), 7.29 (t, *J* = 8.14 Hz, 1H), 7.43–7.46 (m, 1H), 7.53 (t, *J* = 2.20 Hz, 1H), 8.07–8.11 (m, 2H), 8.66–8.69 (m, 2H), 9.29 (s, 1H), 9.63 (s, 1H), 10.59 (s, 1H) ppm; MS (DCI/NH₃) *m/z* 359 (M+H)⁺; Anal. (C₂₁H₁₈N₄O₂) C, H, N.

6.7.7.1. *N*-(3,5-Dimethoxyphenyl)-6-(4-chlorophenyl)-pyrazine-2-carboxamide (15). Yield 75%; mp 156–157 °C; ¹H NMR (DMSO-*d*₆, 300 MHz) δ 3.77 (s, 6H), 6.35 (t, 1H, *J* = 2.1 Hz), 7.20 (d, 2H, *J* = 2.0 Hz), 7.67 (d, 2H, *J* = 8.8 Hz), 8.49 (d, 2H, *J* = 8.8 Hz), 9.23 (s, 1H), 9.54 (s, 1H), 10.53 (s, 1H). MS (ESI) *m/z* 370 (M+H)⁺; Anal. (C₁₉H₁₆ClN₃O₃·0.3 H₂O) C, H, N.

6.7.7.2. *N*-(*m*-Tolyl)-6-(4-chlorophenyl)-pyrazine-2-carboxamide (16). Purified by preparative HPLC on a Waters Nova-Pak[®] HR C18 Prep-Pak[®] cartridge column (40 mm \times 100 mm) using a gradient of 10–100% acetonitrile in 0.1% aqueous TFA over 12 min at a flow rate of 70 mL/min to provide the title compound: mp 136–137 °C; ¹H NMR (DMSO-*d*₆, 300 MHz) δ 3.35 (s, 3H), 7.01 (d, 1H, *J* = 7.5 Hz), 7.30 (t, 1H, *J* = 8.50 Hz), 7.67 (d, 1H, *J* = 8.8 Hz), 7.66–7.77 (m, 3H), 8.51 (d, 2H, *J* = 8.5 Hz), 9.23 (s, 1H), 9.54 (s, 1H), 10.55 (s, 1H). MS (ESI) *m/z* 324 (M+H)⁺; Anal. (C₁₈H₁₄ClN₃O·0.4 TFA) C, H, N.

6.7.7.3. *N*-(3,5-Dimethylphenyl)-6-(4-chlorophenyl)-pyrazine-2-carboxamide (17). Purified by preparative HPLC on a Waters Nova-Pak[®] HR C18 Prep-Pak[®] cartridge column (40 mm \times 100 mm) using a gradient of 10–100% acetonitrile in 0.1% aqueous TFA over 12 min at a flow rate of 70 mL/min to provide the title compound: yield 78%; mp 164 °C; ¹H NMR (DMSO-*d*₆, 300 MHz) δ 2.31 (s, 6H), 6.85–6.82 (m, 1H), 7.52 (s, 2H), 7.67 (d, 2H, *J* = 8.8 Hz), 8.52 (d, 2H, *J* = 8.8 Hz), 9.22 (s, 1H), 9.54 (s, 1H), 10.47 (s, 1H). MS (ESI) *m/z* 338 (M+H)⁺; Anal. (C₁₉H₁₆ClN₃O·0.1 TFA) C, H, N.

6.7.7.4. *N*-(2-Methylbenzyl)-6-(4-chlorophenyl)-pyrazine-2-carboxamide (18). Yield 86%; mp 178 °C; ¹H NMR (DMSO-*d*₆, 300 MHz) δ 4.56 (d, 2H, *J* = 6.1 Hz), 7.12–7.21 (m, 3H), 7.23–7.29 (m, 1H), 7.63 (d, 2H, *J* = 8.6 Hz), 8.46 (d, 2H, *J* = 8.5 Hz), 9.51 (s, 1H), 9.54 (t, 1H, *J* = 6.4 Hz). MS (ESI) *m/z* 338 (M+H)⁺; Anal. (C₁₉H₁₆ClN₃O) C, H, N.

6.7.7.5. *N*-(4-Chlorophenethyl)-6-(4-chlorophenyl)pyrazine-2-carboxamide (19). Yield 89%; mp 157 °C; ¹H NMR (DMSO-*d*₆, 300 MHz) δ ppm 2.91 (t, *J* = 7.5 Hz, 2H), 3.54–3.63 (m, 2H), 7.28–7.39 (m, 4H), 7.65 (d, *J* = 8.5 Hz, 2H), 8.42 (d, *J* = 8.5 Hz, 2H), 9.08–9.15 (m, 2H), 9.49 (s, 1H); MS (DCI/NH₃) *m/z* 372 (M+H)⁺; Anal. (C₁₉H₁₅Cl₂N₃O) C, H, N.

6.7.7.6. *N*-(Pyridin-3-yl)-6-(4-chlorophenyl)-pyrazine-2-carboxamide (20). Yield 49%; mp 213–215 °C; ¹H NMR (DMSO-*d*₆, 300 MHz) δ ppm 7.47 (dd, *J* = 8.1, 4.7 Hz, 1H), 7.61–7.78 (m, 2H), 8.28 (ddd, *J* = 8.3, 2.4, 1.5 Hz, 1H), 8.40 (dd, *J* = 4.7, 1.4 Hz, 1H), 8.48–8.57 (m, 2H), 9.04 (d, *J* = 2.4 Hz, 1H), 9.25 (s, 1H), 9.57 (s, 1H), 10.85 (s, 1H); MS (DCI/NH₃) *m/z* 311 (M+H)⁺; Anal. (C₁₆H₁₁ClN₄O·0.75 H₂O) C, H, N.

6.7.7.7. *N*-(Pyridin-3-ylmethyl)-6-(4-chlorophenyl)-pyrazine-2-carboxamide (21). Yield 56%; mp 167–168 °C; ¹H NMR (DMSO-*d*₆, 300 MHz) δ ppm 4.60 (d, *J* = 6.4 Hz, 2H), 7.36 (ddd, *J* = 7.8, 4.7,

0.7 Hz, 1H), 7.59–7.71 (m, 2H), 7.77 (ddd, $J = 7.8, 2.4, 1.7$ Hz, 1H), 8.42–8.49 (m, 3H), 8.60 (d, $J = 1.7$ Hz, 1H), 9.15 (s, 1H), 9.51 (s, 1H), 9.71 (t, $J = 6.3$ Hz, 1H); MS (DCI/NH₃) m/z 325 (M+H)⁺; Anal. (C₁₇H₁₃ClN₄O·0.7 H₂O) C, H, N.

6.7.7.8. N-((2-Morpholin-4-yl-pyridin-3-yl)methyl)-6-(4-chlorophenyl)-pyrazine-2-carboxamide (22). Yield 40%; mp 140 °C; ¹H NMR (DMSO-*d*₆, 300 MHz) δ ppm 3.06–3.12 (m, 4H), 3.75–3.81 (m, 4H), 4.62 (d, $J = 6.1$ Hz, 2H), 7.03 (dd, $J = 7.5, 4.7$ Hz, 1H), 7.58–7.66 (m, 3H), 8.20 (dd, $J = 4.9, 1.9$ Hz, 1H), 8.47 (d, $J = 8.8$ Hz, 2H), 9.17 (s, 1H), 9.53 (s, 1H), 9.67 (t, $J = 6.1$ Hz, 1H). MS (ESI) m/z 410 (M+H)⁺; Anal. (C₂₁H₂₀ClN₅O₂·0.2 H₂O) C, H, N.

6.7.7.9. N-((3-Morpholinopyridin-4-yl)methyl)-6-(4-chlorophenyl)-pyrazine-2-carboxamide (23). Yield 60%; mp 93–95 °C; ¹H NMR (DMSO-*d*₆, 300 MHz) δ ppm 2.98–3.07 (m, 4H), 3.72–3.87 (m, 4H), 4.68 (d, $J = 6.4$ Hz, 2H), 7.26 (d, $J = 5.1$ Hz, 1H), 7.55–7.74 (m, 2H), 8.26 (d, $J = 5.1$ Hz, 1H), 8.39 (s, 1H), 8.44–8.53 (m, 2H), 9.16 (s, 1H), 9.54 (s, 1H), 9.70 (t, $J = 6.3$ Hz, 1H); MS (DCI/NH₃) m/z 410 (M+H)⁺; Anal. (C₂₁H₂₀ClN₅O₂·0.25 H₂O) C, H, N.

6.7.7.10. N-((4-Morpholinopyridin-3-yl)methyl)-6-(4-chlorophenyl)-pyrazine-2-carboxamide (24). Yield 45%; mp 165–167 °C; ¹H NMR (DMSO-*d*₆, 300 MHz) δ ppm 3.36–3.42 (m, 4H), 3.64–3.70 (m, 4H), 4.44 (d, $J = 6.1$ Hz, 2H), 6.81 (d, $J = 8.8$ Hz, 1H), 7.59 (dd, $J = 8.8, 2.4$ Hz, 1H), 7.61–7.67 (m, 2H), 8.16 (d, $J = 2.0$ Hz, 1H), 8.39–8.48 (m, 2H), 9.13 (s, 1H), 9.49 (s, 1H), 9.55 (t, $J = 6.3$ Hz, 1H); MS (DCI/NH₃) m/z 410 (M+H)⁺; Anal. (C₂₁H₂₀ClN₅O₂·0.1 H₂O) C, H, N.

6.7.7.11. N-((2-Pyrrolidin-1-yl-pyridin-3-yl)methyl)-6-(4-chlorophenyl)-pyrazine-2-carboxamide (25). mp 160–161 °C; ¹H NMR (DMSO-*d*₆, 300 MHz) δ ppm 1.86–1.93 (m, 4H), 3.46–3.52 (m, 4H), 4.60 (d, $J = 6.1$ Hz, 2H), 6.72 (dd, $J = 7.5, 4.7$ Hz, 1H), 7.45 (dd, $J = 7.5, 1.7$ Hz, 1H), 7.63 (d, $J = 8.8$ Hz, 2H), 8.01 (dd, $J = 4.7, 2.0$ Hz, 1H), 8.46 (d, $J = 8.8$ Hz, 2H), 9.15 (s, 1H), 9.52 (s, 1H), 9.55 (t, $J = 6.4$ Hz, 1H). MS (ESI) m/z 394 (M+H)⁺; Anal. (C₂₁H₂₀ClN₅O·0.4 H₂O) C, H, N.

6.7.7.12. N-(3,5-Dimethylphenyl)-6-(4-ethoxyphenyl)-pyrazine-2-carboxamide (26). Yield 44%; mp 162–163 °C; ¹H NMR (DMSO-*d*₆, 300 MHz) δ ppm 1.38 (t, $J = 7.0$ Hz, 3H), 2.30 (s, 6H), 4.15 (q, $J = 7.1$ Hz, 2H), 6.83 (s, 1H), 7.12 (d, $J = 8.8$ Hz, 2H), 7.53 (s, 2H), 8.42 (d, $J = 8.8$ Hz, 2H), 9.12 (s, 1H), 9.45 (s, 1H), 10.42 (s, 1H). MS (DCI/NH₃) m/z 348 (M+H)⁺; Anal. (C₂₁H₂₁N₃O₂·0.8 H₂O) C, H, N.

6.7.7.13. N-(*m*-Tolyl)-6-(4-ethoxyphenyl)-pyrazine-2-carboxamide (27). Yield 46%; mp 152 °C; ¹H NMR (DMSO-*d*₆, 300 MHz) δ ppm 1.38 (t, $J = 7.0$ Hz, 3H), 2.35 (s, 3H), 4.15 (q, $J = 6.9$ Hz, 2H), 7.00 (d, $J = 7.8$ Hz, 1H), 7.12 (d, $J = 8.8$ Hz, 2H), 7.25–7.33 (m, 1H), 7.67–7.74 (m, 2H), 8.42 (d, $J = 8.8$ Hz, 2H), 9.12 (s, 1H), 9.46 (s, 1H), 10.50 (s, 1H). MS (DCI/NH₃) m/z 334 (M+H)⁺; Anal. (C₂₀H₁₉N₃O₂·0.4 H₂O) C, H, N.

6.7.7.14. N-(2-Methylbenzyl)-6-(4-ethoxyphenyl)-pyrazine-2-carboxamide (28). Purified by preparative HPLC; yield 51%; mp 128 °C; ¹H NMR (DMSO-*d*₆, 300 MHz) δ ppm 1.37 (t, $J = 7.0$ Hz, 3H), 2.36 (s, 3H), 4.13 (q, $J = 6.9$ Hz, 2H), 4.56 (d, $J = 6.4$ Hz, 2H), 7.09 (d, $J = 9.2$ Hz, 2H), 7.12–7.21 (m, 3H), 7.23–7.29 (m, 1H), 8.36 (d, $J = 8.8$ Hz, 2H), 9.05 (s, 1H), 9.42 (d, $J = 0.7$ Hz, 1H), 9.46 (t, $J = 6.3$ Hz, 1H); MS (ESI) m/z 348 (M+H)⁺; Anal. (C₂₁H₂₁N₃O₂·0.16 TFA) C, H, N.

6.7.7.15. N-(3,5-Dimethylphenyl)-6-(4-cyanophenyl)-pyrazine-2-carboxamide (29). Yield 86%; mp 167–168 °C; ¹H NMR (DMSO-*d*₆, 300 MHz) δ 2.31 (s, 6H), 6.84 (s, 1H), 7.52 (s, 2H),

8.07–8.10 (m, 2H), 8.67–8.70 (m, 2H), 9.28 (s, 1H), 9.62 (s, 1H), 10.51 (s, 1H) ppm. MS (DCI/NH₃) m/z 329 (M+H)⁺; Anal. (C₂₀H₁₆N₄O) C, H, N.

6.7.7.16. N-(3,5-Dimethylphenyl)-6-(4-trifluoromethoxyphenyl)-pyrazine-2-carboxamide (32). Yield 65%; mp 135–136 °C; ¹H NMR (DMSO-*d*₆, 300 MHz) δ 2.30 (s, 6H), 6.83 (s, 1H), 7.52 (s, 2H), 7.58–7.60 (m, 2H), 8.57–8.62 (m, 2H), 9.24 (s, 1H), 9.55 (s, 1H), 10.47 (s, 1H) ppm. MS (DCI/NH₃) m/z 388 (M+H)⁺; Anal. (C₂₀H₁₆F₃N₃O₂) C, H, N.

6.7.7.17. N-(*m*-Tolyl)-6-(4-trifluoromethoxyphenyl)-pyrazine-2-carboxamide (33). Purified by preparative HPLC; yield 79%; mp 124–125 °C; ¹H NMR (DMSO-*d*₆, 300 MHz) δ 2.35 (s, 3H), 7.00–7.02 (m, 1H), 7.27–7.33 (m, 1H), 7.58–7.61 (m, 2H), 7.69–7.72 (m, 2H), 8.57–8.62 (m, 2H), 9.25 (s, 1H), 9.55 (s, 1H), 10.56 (s, 1H) ppm. MS (DCI/NH₃) m/z 374 (M+H)⁺; Anal. (C₁₉H₁₄F₃N₃O₂·0.08 TFA) C, H, N.

6.7.7.18. N-((2-Chloropyridin-3-yl)methyl)-6-(4-(trifluoromethoxy)phenyl)pyrazine-2-carboxamide (35). Yield 27%; mp 137–138 °C; ¹H NMR (DMSO-*d*₆, 300 MHz) δ 4.64 (d, $J = 6.10$ Hz, 2H), 7.42 (dd, $J = 7.80, 4.75$ Hz, 1H), 7.58, (d, $J = 7.80$ Hz, 2H), 7.80 (dd, $J = 7.63, 1.86$ Hz, 1H), 8.33 (dd, $J = 4.75, 1.70$ Hz, 1H), 8.53–8.58 (m, 2H), 9.17 (s, 1H), 9.55 (s, 1H), 9.72 (t, $J = 6.10$ Hz, 1H) ppm. MS (DCI/NH₃) m/z 409 (M+H)⁺; Anal. (C₁₈H₁₂ClF₃N₄O₂·0.18 H₂O) C, H, N.

6.7.7.19. N-((2-Morpholin-4-yl-pyridin-3-yl)methyl)-6-(4-cyanophenyl)-pyrazine-2-carboxamide (36). Yield 94%; mp 98–99 °C; ¹H NMR (DMSO-*d*₆, 400 MHz) δ 3.07–3.09 (m, 4H), 3.75–3.77 (m, 4H), 4.62 (d, $J = 5.83$ Hz, 2H), 7.01 (dd, $J = 7.52, 4.60$ Hz, 1H), 7.50–7.52 (m, 2H), 7.61 (d, $J = 7.36$ Hz, 1H), 8.81 (d, $J = 4.60$ Hz, 1H), 8.51–8.53 (m, 2H), 9.17 (s, 1H), 9.50 (s, 1H), 9.64 (t, $J = 6.14$ Hz, 1H) ppm. MS (DCI/NH₃) m/z 460 (M+H)⁺; Anal. (C₂₂H₂₀F₃N₅O₃) C, H, N.

6.7.8. Representative procedure for amide formation from methyl esters (Scheme 4, step a). N-(2-Methylbenzyl)-6-(4-cyanophenyl)-pyrazine-2-carboxamide (31)

Methyl 6-(4-cyanophenyl)-2-pyrazinecarboxylate (**5**) (71.6 mg, 0.30 mmol) and MgCl₂ (62.4 mg, 0.66 mmol) were suspended in THF (3 mL) and stirred at ambient temperature for 5 min. 2-Methylbenzylamine (100 μ L, 0.81 mmol) was added and the reaction mixture was stirred at 40 °C for 4 h. The solid material was removed by filtration and washed with CH₂Cl₂ (3 \times 2 mL). The combined filtrates were concentrated and purified by preparative HPLC; yield 64%; mp 161 °C; ¹H NMR (DMSO-*d*₆, 300 MHz) δ 2.36 (s, 3H), 4.57 (d, $J = 6.44$ Hz, 2H), 7.13–7.28 (m, 4H), 8.05–8.08 (m, 2H), 8.63–8.65 (m, 2H), 9.22 (s, 1H), 9.57–9.61 (m, 2H) ppm; MS (DCI/NH₃) m/z 329 (M+H)⁺; Anal. (C₂₀H₁₆N₄O·0.04 TFA) C, H, N.

6.7.8.1. N-(2-Methylbenzyl)-6-(4-trifluoromethoxyphenyl)-pyrazine-2-carboxamide (32). Purified by preparative HPLC; yield 79%; mp 130 °C; ¹H NMR (DMSO-*d*₆, 300 MHz) δ 2.36 (s, 3H), 4.56 (d, $J = 6.44$ Hz, 2H), 7.12–7.28 (m, 4H), 7.55–7.58 (m, 2H), 8.52–8.57 (m, 2H), 9.17 (s, 1H), 9.52–9.56 (m, 2H) ppm; MS (DCI/NH₃) m/z 388 (M+H)⁺; Anal. (C₂₀H₁₆F₃N₃O₂) C, H, N, F.

References and notes

- Anger, T.; Madge, D. J.; Mulla, M.; Riddall, D. J. *Med. Chem.* **2001**, *44*, 115.
- Goldin, A. L.; Barchi, R. L.; Caldwell, J. H.; Hofmann, F.; Howe, J. R.; Hunter, J. C.; Kallen, R. G.; Mandel, G.; Meisler, M. H.; Netter, Y. B.; Noda, M.; Tamkun, M. M.; Waxman, S. G.; Wood, J. N.; Catterall, W. A. *Neuron* **2000**, *28*, 365.
- Catterall, W. A.; Goldin, A. L.; Waxman, S. G. *Pharmacol. Rev.* **2005**, *57*, 397.
- Catterall, W. A. *Neuron* **2000**, *26*, 13.

5. Lai, J.; Porreca, F.; Hunter, J. C.; Gold, M. S. *Annu. Rev. Pharmacol. Toxicol.* **2004**, *44*, 371.
6. Wood, J. N.; Boorman, J. *Curr. Top. Med. Chem.* **2005**, *5*, 529.
7. Lai, J.; Hunter, J. C.; Porreca, F. *Curr. Opin. Neurobiol.* **2003**, *13*, 291.
8. Waxman, S. G.; Cummins, T. R.; Dib-Hajj, S.; Fjell, J.; Black, J. A. *Muscle Nerve* **1999**, *22*, 1177.
9. Kinloch, R. A.; Cox, P. J. *Expert Opin. Ther. Targets* **2005**, *9*, 685.
10. Renganathan, M.; Cummins, T. R.; Waxman, S. G. *J. Neurophysiol.* **2001**, *86*, 629.
11. Lai, J.; Gold, M. S.; Kim, C.-S.; Bian, D.; Ossipov, M. H.; Hunter, J. C.; Porreca, F. *Pain* **2002**, *95*, 143.
12. Amir, R.; Argoff, C. E.; Bennett, G. J.; Cummins, T. R.; Durieux, M. E.; Gerner, P.; Gold, M. S.; Porreca, F.; Strichartz, G. R. *J. Pain* **2006**, *7*, S1.
13. Coggeshall, R. E.; Tate, S.; Carlton, S. M. *Neurosci. Lett.* **2004**, *355*, 45.
14. Laird, J. M. A.; Souslova, V.; Wood, J. N.; Certero, F. *J. Neurosci.* **2002**, *22*, 8352.
15. Nassar, M. A.; Levato, A.; Stirling, L. C.; Wood, J. N. *Mol. Pain* **2005**, *1*, 24.
16. Akopian, A. N.; Souslova, V.; England, S.; Okuse, K.; Ogata, N.; Ure, J.; Smith, A.; Kerr, B. J.; McMahon, S. B.; Boyce, S.; Hill, R.; Stanfa, L. C.; Dickenson, A. H.; Wood, J. N. *Nat. Neurosci.* **1999**, *2*, 541.
17. Gold, M. S.; Weinreich, D.; Kim, C.-S.; Wang, R.; Treanor, J.; Porreca, F.; Lai, J. *J. Neurosci.* **2003**, *23*, 158.
18. Joshi, S. K.; Mikusa, J. P.; Hernandez, G.; Baker, S.; Shieh, C. C.; Neelands, T.; Zhang, X.; Niforatos, W.; Kage, K.; Han, P.; Krafft, D.; Faltynek, C.; Sullivan, J. P.; Jarvis, M. F.; Honore, P. *Pain* **2006**, *123*, 75.
19. Porreca, F.; Lai, J.; Bian, D.; Wegert, S.; Ossipov, M. H.; Eglén, R. M.; Kassotakis, L.; Novakovic, S.; Rabert, D. K.; Sangameswaran, L.; Hunter, J. C. *Proc. Natl. Acad. Sci. U.S.A.* **1999**, *96*, 7640.
20. Kalso, E. *Curr. Pharm. Des.* **2005**, *11*, 3005.
21. Priestley, T. *Curr. Drug Targets: CNS Neurol. Disord.* **2004**, *3*, 441.
22. Weiser, T. *Drugs Future* **2006**, *31*, 597.
23. Matelenko, M. A.; Scanio, M. J. C.; Kort, M. E. *Curr. Top. Med. Chem.* **2009**, *9*, 362.
24. Kort, M. E.; Drizin, I.; Gregg, R. J.; Scanio, M. J. C.; Shi, L.; Gross, M. F.; Atkinson, R. N.; Johnson, M. S.; Pacofsky, G. J.; Thomas, J. B.; Carroll, W. A.; Krambis, M. J.; Liu, D.; Shieh, C.-C.; Zhang, X.; Hernandez, G.; Mikusa, J. P.; Zhong, C.; Joshi, S.; Honore, P.; Roeloffs, R.; Marsh, K. C.; Murray, B. P.; Liu, J.; Werness, S.; Faltynek, C. R.; Krafft, D. S.; Jarvis, M. F.; Chapman, M. L.; Marron, B. E. *J. Med. Chem.* **2008**, *51*, 407.
25. Jarvis, M. F.; Honore, P.; Shieh, C. C.; Chapman, M.; Joshi, S. K.; Zhang, X. F.; Kort, M. E.; Carroll, W. A.; Marron, B. E.; Atkinson, R. N.; Thomas, J. B.; Liu, D.; Krambis, M. J.; Liu, Y.; McGaraughty, S.; Chu, K.; Roeloffs, C. R.; Zhong, C.; Mikusa, J. P.; Hernandez, G.; Gauvin, D.; Wade, C.; Zhu, C.; Pai, M.; Scanio, M. J. C.; Shi, L.; Drizin, I.; Gregg, R. J.; Matulencko, M. A.; Ahmed Hakeem, A. H.; Gross, M. F.; Johnson, M. S.; Marsh, K. C.; Wagoner, K.; Sullivan, J. P.; Faltynek, C. R.; Krafft, D. S. *Proc. Natl. Acad. Sci. U.S.A.* **2007**, *104*, 8520.
26. McGaraughty, S.; Chu, K. L.; Scanio, M. J. C.; Kort, M. E.; Faltynet, C. R.; Jarvis, M. F. *J. Pharm. Exp. Ther.* **2008**, *324*, 1204.
27. Kort, M. E.; Atkinson, R. N.; Thomas, J. B.; Drizin, I.; Johnson, M. S.; Secrest, M. A.; Gregg, R. J.; Scanio, M. J. C.; Shi, L.; Hakeem, A. H.; Matulencko, M. A.; Chapman, M. L.; Krambis, M. J.; Liu, D.; Shieh, C.-C.; Zhang, X.; Hernandez, G.; Mikusa, J. P.; Zhong, C.; Joshi, S.; Honore, P.; Roeloffs, R.; Werness, S.; Antonio, B.; Marsh, K. C.; Faltynek, C. R.; Krafft, D. S.; Jarvis, M. F.; Marron, B. E. *Bioorg. Med. Chem. Lett.* **2010**. doi:10.1016/j.bmcl.2010.08.121.
28. Uchimaru, F.; Okada, S.; Kosasayama, A.; Konno, T. *Chem. Pharm. Bull.* **1971**, *19*, 1337.
29. Okada, S.; Kosasayama, A.; Konno, T.; Uchimaru, F. *Chem. Pharm. Bull.* **1971**, *19*, 1344.
30. Imai, K.-I.; Mano, M.; Seo, T.; Matsuno, T. *Chem. Pharm. Bull.* **1981**, *29*, 88.
31. Sato, N.; Fujii, M. *J. Heterocycl. Chem.* **1994**, *31*, 1177.
32. Guo, Z.; Dowdy, E. D.; Li, W.-S.; Polniaszek, R.; Delaney, E. *Tetrahedron Lett.* **2001**, *42*, 1843.
33. Daniel, S.; Malkowitz, L.; Wang, H.-C.; Beer, B.; Blume, A. J.; Ziai, M. R. *J. Pharmacol. Meth.* **1991**, *25*, 185.
34. Tang, W.; Kang, J.; Wu, X.; Rampe, D.; Wang, L.; Shen, H.; Li, Z.; Dunnington, D.; Garyantes, T. *J. Biomol. Screen.* **2001**, *6*, 325.
35. Joshi, S. K.; Honore, P. *Expert Opin. Drug Disc.* **2006**, *1*, 323.
36. Worley, J. F.; Main, M. J. *Receptors Channels* **2002**, *8*, 269.
37. Jarvis, M. F.; Burgard, E. C.; McGaraughty, S.; Honore, P.; Lynch, K.; Brennan, T. J.; Subieta, A.; Van Biesen, T.; Cartmell, J.; Bianchi, B.; Niforatos, W.; Kage, K.; Yu, H.; Mikusa, J.; Wismer, C. T.; Zhu, C. Z.; Chu, K.; Lee, C. H.; Stewart, A. O.; Polakowski, J.; Cox, B. F.; Kowaluk, E.; Williams, M.; Sullivan, J.; Faltynek, C. *Proc. Natl. Acad. Sci. U.S.A.* **2002**, *99*, 17179.
38. Zhang, X. F.; Zhu, C. Z.; Thimmapaya, R.; Choi, W. S.; Honore, P.; Scott, V. E.; Kroeger, P. E.; Sullivan, J. P.; Faltynek, C. R.; Gopalakrishnan, M.; Shieh, C. C. *Brain Res.* **2004**, *1009*, 147.
39. Joshi, S. K.; Hernandez, G.; Mikusa, J. P.; Zhu, C. Z.; Zhong, C.; Salyers, A.; Wismer, C. T.; Chandran, P.; Decker, M. W.; Honore, P. *Neuroscience* **2006**, *143*, 587.
40. Kim, S. H.; Chung, J. M. *Pain* **1992**, *50*, 355.